1 Introduction

Intuition about the relationship between tectonic and geomorphic processes and the resulting topography may be built by combining detailed field observations with careful theoretical analysis. While detailed observations are commonly the cornerstone of sound geologic studies, theoretical modelling of the processes involved that produce the observations is often impaired by the inability to solve the governing equations of these processes for typical geologic conditions. However, numerical methods may be employed that let us approximate the governing differential equations for a wide range of geologically applicable scenarios.

This section describes and illustrates a simple implementation of the Finite Difference Method (FDM) for investigating the development of hillslope topography. Using this numerical technique, we show how simple ideas about the transport of geomorphic material, production of regolith from bedrock, and relative tectonic displacements may be used to extrapolate limited observations of topography at a particular time to approximations of how the topography might have looked in the past and future. In addition, conceptual models, cast in the language of mathematics, allow us to link observations that typically do not directly tell us about the underlying processes to the processes themselves. This portion of the document is modified from Arrowsmith, 1995.

2 Diffusive Hillslope Transport

2.1 Review of basic derivation

We use for our example of the finite difference method a hillslope whose transport is governed only by the local slope and some transport constant and for which conditions are transport-limited. This situation is described in a previous section, and results in the following governing differential equation for material transport:

$$Q(x) = -\kappa \frac{\partial H}{\partial x} \tag{1}$$

Where x is the location of each point along the profile, H is the elevation at that point, κ is the hillslope diffusivity, and $Q(x)$ is the flux of material at each point.

In addition, if the density of sediment remains constant through transport, any change in flux must be compensated by either 1) the addition or removal of material at each point, or 2) a change in the elevation. This mass balance can be expressed in the form of the continuity equation:

$$\frac{\partial H}{\partial t} = -\frac{\partial Q}{\partial x} \tag{2}$$

These two equations constitute the constitutive equations of diffusive hillslope erosion. Substitute the transport rule (1 for $Q(x)$ into the continuity equation (2) to get the homogeneous linear diffusion equation in which the change in

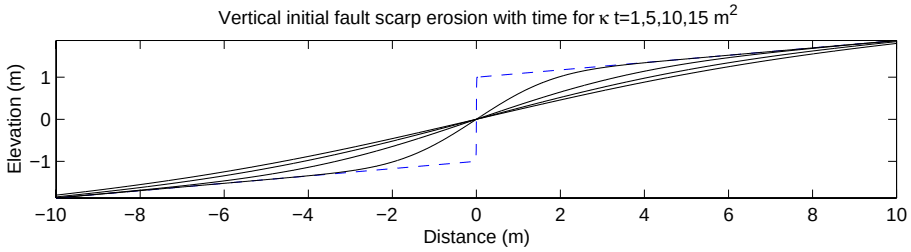

Figure 1: The geometry of a simple initially vertical fault scarp and its subsequent degradation with time. Dashed line is the initially vertical profile, the initial offset ($2a$) is 2 m, and $b = 5°$.

elevation with time is proportional to the local curvature of the topographic profile:

$$\frac{\partial H}{\partial t} = \kappa \frac{\partial^2 H}{\partial x^2} \tag{3}$$

3 is analogous to the heat conduction equation for one dimensional heat transport in which κ would be the coefficient of proportionality called the thermal conductivity and H would be temperature (e.g., Avouac, 1993; Hanks et al., 1984; Nash, 1980).

2.2 Analytical solutions to the diffusion equation–Vertical scarp initial conditions

First, we will illustrate the analytic solutions to the simple diffusion equation (an approach presented in Hanks et al., 1984). A solution of the homogeneous linear diffusion equation (3) for a step of topography of $2a$ at $t = 0$ and $x = 0$ (e.g., a newly formed fault scarp, and note that the origin for x in this example is in the mid scarp and not at the upper boundary) on a pre-existing topographic slope of b is

$$H(x,t) = a \ \mathrm{erf}\left(\frac{x}{2\sqrt{kt}}\right) + bx \tag{4}$$

The resulting profiles are not uniquely dependent on t or κ, but rather their product. For example, the same profile will result for $\kappa = 1$ m^2/kyr and $t = 10$ kyr or $\kappa = 10$ m^2/kyr and $t = 1$ kyr. (T. C. Hanks personal communication and Hanks et al., 1984). For this presentation, we have separated these values to emphasize the fact that a known value for κ or t may be used to constrain the other. Figure 1 shows the geometry of this simple fault scarp and a graphical solution to 4 for a step of 2 m at time zero and a far field or fan slope of 5°, and its subsequent degradation with time.

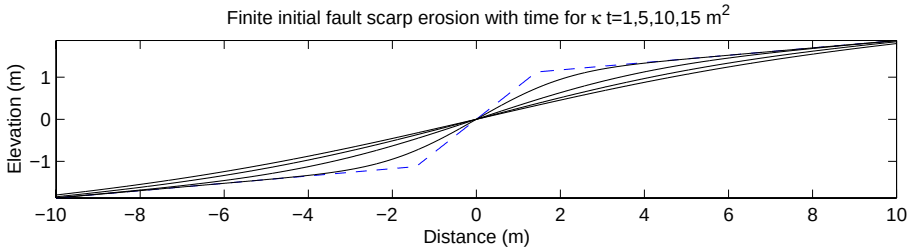

Figure 2: The geometry of a finite initial slope fault scarp and its subsequent degradation with time. Dashed line is the initial profile (initial scarp slope of 45°), the initial offset ($2a$) is 2 m, and $b = 5°$.

2.3 Analytical solutions to the diffusion equation–Finite slope scarp initial conditions

Equation 4 provided a solution of the diffusion equation (3) for an infinite slope (vertical) initial scarp slope (Figure 1). Clearly, a vertical scarp will not last long, nor will "diffusive" processes operate on such steep slopes. Therefore, it is important to develop the analysis for finite initial slope scarps. Hanks and Andrews (1989) provided the following equation for the same conditions that give rise to 4, except that the fault "occurs" on a slope of θ instead of ∞. The solution to 3 is:

$$H(x,t) = (\theta - b)\left(\frac{\kappa t}{\pi}\right)^{1/2}\left\{\exp\left(-\frac{x + a/(\theta - b)}{4\kappa t}\right) - \exp\left(-\frac{x - a/(\theta - b)}{4\kappa t}\right)\right\} + \frac{\theta - b}{2}\left\{\left(x + \frac{a}{\theta - b}\right)\mathrm{erf}\left(\frac{x + a/(\theta - b)}{(4\kappa t)^{1/2}}\right) - \left(x - \frac{a}{\theta - b}\right)\mathrm{erf}\left(\frac{x - a/(\theta - b)}{(4\kappa t)^{1/2}}\right)\right\} + bx \quad (5)$$

Figure 2 shows the geometry of this simple fault scarp and a graphical solution to 5 for a step of 2 m at time zero and a far field or fan slope of 5°, and a finite initial scarp slope of 45°, and its subsequent degradation with time.

The *MATLAB* codes for solving these equations are available at
`http://activetectonics.la.asu.edu/diffuse/`

For some specific initial and boundary conditions, analytic solutions such as those presented in this and the last section may be solved (e.g., Carslaw and Jaeger, 1959 and see Hanks, 2000 and references therein). However, in many geologic environments, initial profiles may be complicated. Also, tectonic displacements will not be uniform, as points near the fault ends will have different displacements than their counterpoints located far from these ends. Finally, fault slip rates may vary with time and geomorphic transport may be subject to certain constraints, such as the lack of transportable material once bedrock

is exposed. For this reason, flexible numerical solutions to these differential equations are necessary if we are to apply the principles of this simple transport process to a wide range of realistic geologic conditions.

3 Finite difference approximation

3.1 Taylor series and approximations of the first derivative

The finite difference method is based on the idea that derivatives and integrals of functions can be approximated by calculating discrete values of the equations when the differentiation or integration step is small. For example, in the difference quotient, which relates a function to its derivative, we approximate the limit of $dx \to 0$ by letting dx equal some arbitrarily small number. To do this, we first divide the solution space into discrete elements, separated by a uniform, but small distance, Δx. Each point (or node) in this space has a corresponding value of the function. In our example, we consider the location of the nodes to represent the distance along a topographic profile and their values to represent the elevation at a each location. If we need to compute the derivative (or slope) of the topography, we can use the Taylor Series approximation of a function at a point (Chapra and Canale, 1988; Ferziger , 1981):

$$\begin{aligned} f(x_{i+1}) &= f(x_i) + f'(x_i)(x_{i+1} - x_i) + f''\frac{x_i}{2!}(x_{i+1} - x_i)^2 \\ &\quad + f'''\frac{x_i}{3!}(x_{i+1} - x_i)^3 + \ldots + f^n\frac{x_i}{n!}(x_{i+1} - x_i)^n + R_n \end{aligned} \tag{6}$$

where R_n is a remainder term for terms $n+1$ to ∞, and $f'(x_i)$ is the first derivative at x_i, etc. If we assume that the terms to the right of the first derivative that we are trying to compute (f') yield an answer that is small, we can truncate the remaining terms and solve for the value of the derivative:

$$\begin{aligned} f(x_{i+1}) &= f(x_i) + f'(x_i)(x_{i+1} - x_i) + R_1 \\ f'(x_i) &= \frac{f(x_{i+1}) - f(x_i)}{x_{i+1} - x_i} - \frac{R_1}{x_{i+1} - x_i} \\ &\quad \text{(1st order approximation} - \text{truncation error)} \end{aligned} \tag{7}$$

Then let $\Delta x = (x_{i+1} - x_i)$ [step size], and $\Delta f = f(x_{i+1}) - f(x_i)$ [first forward difference], so that the finite divided difference is

$$f'(x_i) = \frac{\Delta f}{\Delta x} - \frac{0}{\Delta x} \tag{8}$$

In the finite difference approach, we assume that the space step is uniform in the model space. Therefore, the denominator of 7 is equal to the uniform spacing (Δx). Importantly, in the above example, we have truncated the trailing terms in the Taylor series approximation, assuming that they are small relative to the

value of the derivative we computed. This is conceptually the simplest way to compute a finite difference, but is definitely not the most accurate. Because only the first term of the Taylor Series was kept in our approximation, we term this method "first-order accurate." Generally, we desire methods that are more accurate than this for our approximations.

In the above derivation, we computed the derivative of the function by using the point located one step beyond the point at which the derivative was calculated. We could have just as easily elected to compute the derivative based on the previous point, located one step behind the point at which we wish to calculate the derivative. The preceding derivation is called the *forward finite difference* because it computes the derivative based on the point ahead of the point of the derivative, and the latter case is called the *backward finite difference*. It is computed in a similar way as the forward finite difference:

$$f(x_{i-1}) = f(x_i) - f'(x_i)\Delta x + f''\frac{\Delta x^2}{2!} - \dots \tag{9}$$

By subtracting these two approximations, a far more accurate approximation (called the *centered finite difference*) of the derivative can be made:

$$\begin{aligned} f(x_{i+1}) &= f(x_{i-1}) + 2f'(x_i)\Delta x + f'''\frac{\Delta x^3}{3!} + \dots \\ f'(x_i) &= \frac{f(x_{i+1}) - f(x_{i-1})}{2\Delta x} - \frac{f'''(x_i)}{6}\Delta x^2 \\ f'(x_i) &= \frac{f(x_{i+1}) - f(x_{i-1})}{2\Delta x} - 0\Delta x^2 \end{aligned} \tag{10}$$

Equation 10 is the centered or central difference representation of the first derivative. Notice that it is second order accurate (we truncate after the second derivative). Figure 3 shows the geometry of these first derivative approximations.

3.2 Finite difference approximations of higher order derivatives

First, write a forward Taylor Series approximation of $f(x_{i+2})$ in terms of $f(x_i)$:

$$f(x_{i+2}) = f(x_i) + f'(x_i)(2\Delta x) + f''\frac{x_i}{2!}2\Delta x^2 + \dots \tag{11}$$

Multiply 8 by 2 and subtract from 11 to yield

$$f(x_{i+2}) - 2f(x_{i+1}) = -f(x_i) + f''\frac{x_i}{2!}2\Delta x^2 + \dots \tag{12}$$

Which is solved for

$$f''(x_i) = \frac{f(x_{i+2}) - 2f(x_{i+1}) + f(x_i)}{\Delta x^2} - \frac{0}{\Delta x} \tag{13}$$

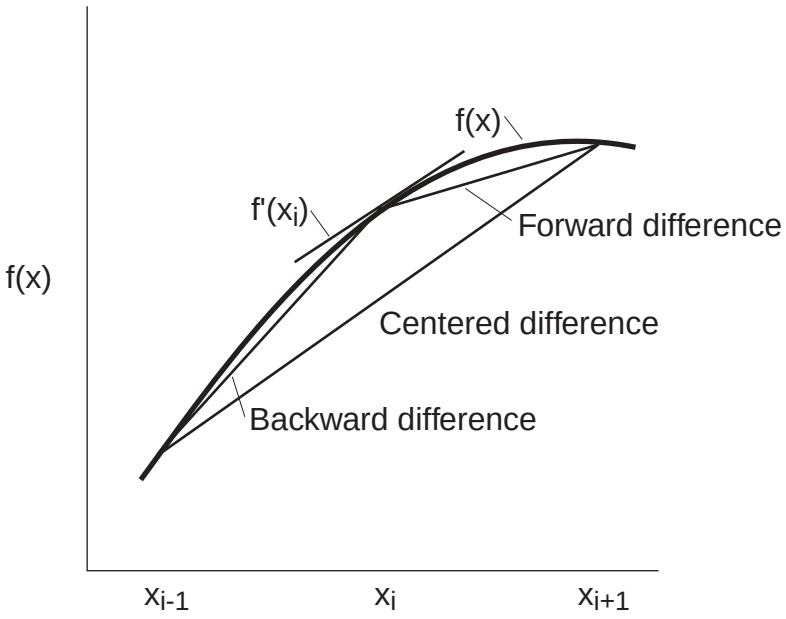

Figure 3: Graphical representation of various difference approximations of the slope (1st derivative; $f'(x_i)$) of a function and their relation to the true slope at that point. Note the increased accuracy of the centered difference.

That relationship is called the *second forward finite divided difference*. Similar manipulations can be employed to derive a backward version

$$f''(x_i) = \frac{f(x_i) - 2f(x_{i-1}) + f(x_{i-2})}{\Delta x^2} - \frac{0}{\Delta x} \tag{14}$$

and a centered version

$$f''(x_i) = \frac{f(x_{i+1}) - 2f(x_i) + f(x_{i-1})}{\Delta x^2} - \frac{0}{\Delta x^2} \tag{15}$$

As was the case with the 1st order approximations, the centered version is more accurate. Also notice that the centered version can alternatively be expressed as

$$f''(x_i) = \frac{\frac{f(x_{i+1}) - f(x_i)}{\Delta x} - \frac{f(x_i) - f(x_{i-1})}{\Delta x}}{\Delta x} - \frac{0}{\Delta x^2} \tag{16}$$

Thus, just as the second derivative is the derivative of a derivative, the second divided difference approximation is a difference of two first divided differences.

4 Numerical solutions to the basic linear diffusion erosion problem

4.1 Derivation

Here we present an explicit finite difference method for solving equation 3 for arbitrary initial conditions (see Figure 4 for the temporal and spatial discretization grid and computational molecule). First, approximate the time derivative (left hand side of 3) with a forward divided difference 8:

$$\frac{\partial H}{\partial t} \approx \frac{H_i^{l+1} - H_i^l}{\Delta t} \tag{17}$$

Note that we introduce the space index i (subscripted) and the time index l (superscripted). We assume no tectonic input and transport-limited conditions. Secondly, approximate the space derivative (right hand side of 3) by a centered divided difference 15:

$$\frac{\partial^2 H}{\partial x^2} \approx \kappa \frac{H_{i+1}^l - 2H_i^l + H_{i-1}^l}{\Delta x^2} \tag{18}$$

substitute 17 and 18 into 3 to yield the explicit finite difference approximation of the elevation at H_i^{l+1} as a function of its neighbor points at H_i^l. It provides an explicit means of computing values at each node for a future time, based on

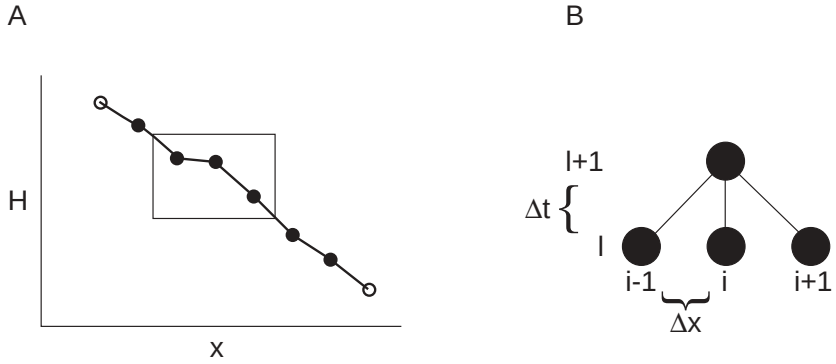

Figure 4: A) Discretized profile. Interior nodes are solid and their changes in elevation with time can be solved with the method described here, whereas the boundary node (open) elevations must always be specified. B) Computational molecule for three adjacent nodes within the profile (for example those boxed at left). Note how the elevation of the central point (i) in the future ($l + 1$) is a function of its elevation and that of its immediate neighbors at time l.

the present values.

$$\begin{aligned} \frac{H_i^{l+1} - H_i^l}{\Delta t} &= \kappa \frac{H_{i+1}^l - 2H_i^l + H_{i-1}^l}{\Delta x^2} \\ H_i^{l+1} &= H_i^l + \frac{\kappa \Delta t}{\Delta x^2} \left(H_{i+1}^l - 2H_i^l + H_{i-1}^l \right) \\ H_i^{l+1} &= H_i^l + \lambda \left(H_{i+1}^l - 2H_i^l + H_{i-1}^l \right) \end{aligned} \tag{19}$$

where $\lambda = \frac{\kappa \Delta t}{\Delta x^2}$. This equation is written for all interior nodes of the profile (Figure 4). This explicit method is convergent and stable for $\lambda \leq 1/2$, or $\Delta t \leq \frac{1}{2} \frac{\Delta x^2}{\kappa}$ (Ferziger, 1981).

4.2 Benchmarking the method–how accurate is it?

Whenever one uses an approximate method such as the FDM discussed here, it is appropriate to check its accuracy by comparing numerical results with those calculated analytically. Such a calculation has to be done within the stricter conditions of the analytical solution, but it lends confidence to the subsequent broader application of the numerical solutions.

As an illustration of the accuracy and behavior of the numerical method employed above, we "benchmarked" it against the finite slope analytical solution (5) for a morphologic age of $\kappa t = 5$ m^2 (Figure 5). In that figure, the upper panel shows that the two methods are graphically similar and that the error is small. The lower panel shows the difference between the analytical and numerical solutions and illustrates two important points: 1) The lower magnitude errors that are antisymmetric about the origin are due to the numerical inaccuracy. They correlate with the curvature of the model. 2) The larger magnitude errors at the end of the profile are the result of a difference between the boundary conditions of the numerical model (constant elevation) and the elevation change calculated analytically. The analytical model indicates that a morphologic age of 5 m^2, elevation change (erosion and deposition) has reached the edges of the solution domain (-10 and 10 m). However, the numerical model fixes those boundary elevations and thus the two solutions diverge. To address this problem, the easiest thing to do is extend the numerical method boundaries far beyond the domain of interest (and increase the number of nodes if the same level of detail in the approximation is desired).

4.3 An example application of the 1-D explicit finite difference method solved using a spreadsheet (Microsoft Excel)

In Figures 6, 7, and 8, we illustrate how one might solve the diffusion erosion problem using a spreadsheet. Figure 6 is an example spreadsheet used to solve 3 by 19. The constants in solid boxes are input, and the spreadsheet determines the rest. Figure 7 shows the necessary Microsoft Excel formulae. In order to calculate to a given age, we must copy the D column to the right enough times

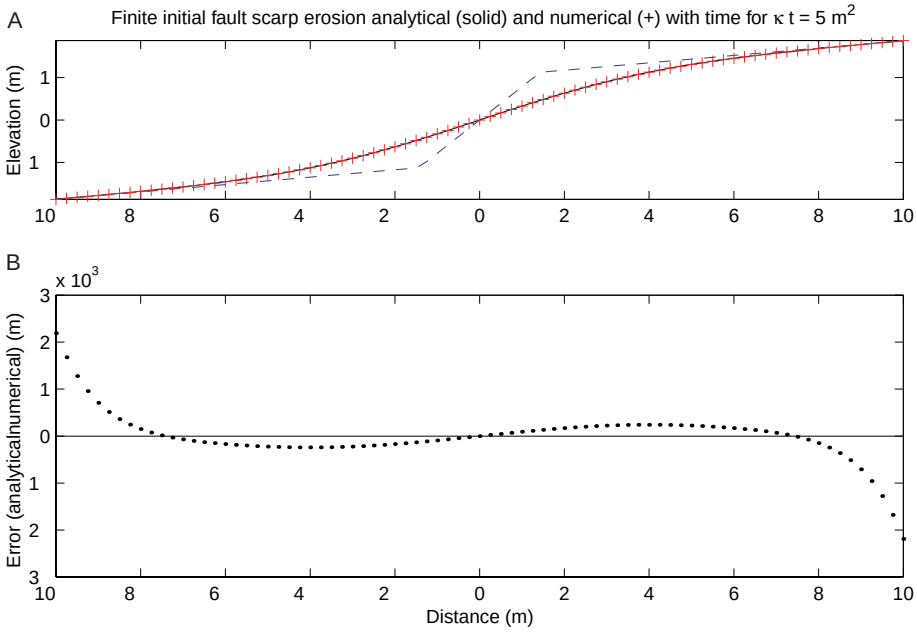

Figure 5: A) Comparison between analytical (solid line) and numerical (+) solutions to the diffusion erosion of the initial profile (dashed line) for $\kappa t = 5$ m^2. B) Difference between analytical and numerical solutions. Errors are acceptably small and in the interior result from numerical inaccuracy and on the edges from the difference in boundary conditions (constant elevation for numerical method and elevation change for analytical method).

to keep the calculation stable. For example, to determine the profile shown in Figure 8A, 100 time steps, or 100 columns were used. For the given parameters such a result is well within the stability criterion (unlike Figure 8B; a nice example of an unstable solution). These examples are limited in number of nodes for convenience. Simple explorations with this tool can be very useful to build intuition about this geomorphic process, the importance of initial and boundary conditions, and the uniqueness of the morphologic age (κt) for form. More elaborate spreadsheets and simple exercises are available at
`http://www.public.asu.edu/~arrows/geomorph/diffuse/index.html`.
A *MATLAB* implementation of this method is available at
`http://activetectonics.la.asu.edu/diffuse/`

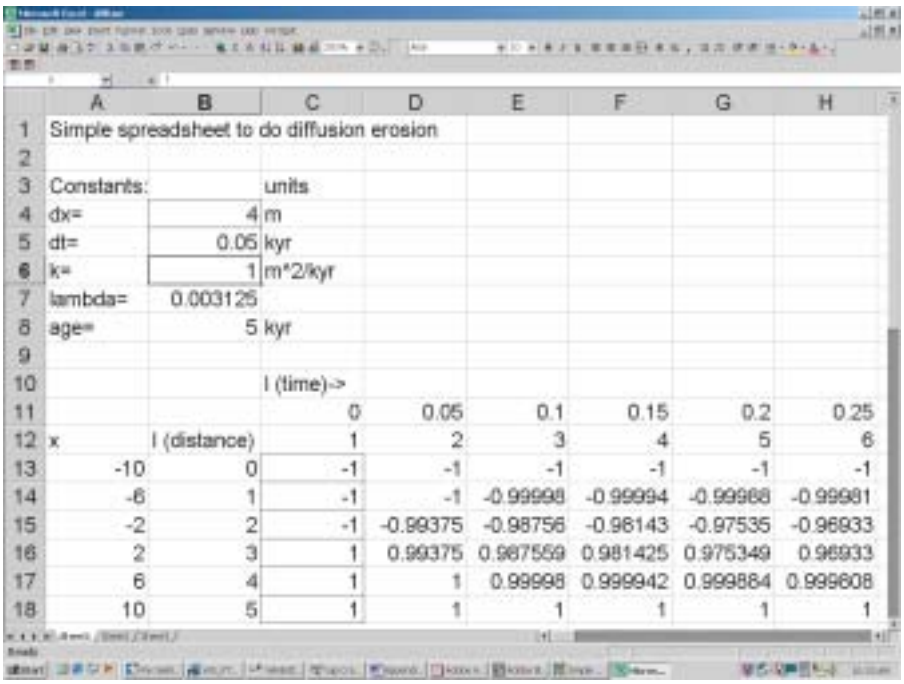

	A	B	C	D	E	F	G	H
1	Simple spreadsheet to do diffusion erosion							
2								
3	Constants:		units					
4	dx=	4	m					
5	dt=	0.05	kyr					
6	k=	1	m^2/kyr					
7	lambda=	0.003125						
8	age=	5	kyr					
9								
10			I (time)->					
11			0	0.05	0.1	0.15	0.2	0.25
12	x	I (distance)	1	2	3	4	5	6
13	-10	0	-1	-1	-1	-1	-1	-1
14	-6	1	-1	-1	-0.99998	-0.99994	-0.99988	-0.99981
15	-2	2	-1	-0.99375	-0.98756	-0.96143	-0.97535	-0.96933
16	2	3	1	0.99375	0.987559	0.981425	0.975349	0.96933
17	6	4	1	1	0.99998	0.999942	0.999884	0.999808
18	10	5	1	1	1	1	1	1

Figure 6: Example Microsoft Excel Spreadsheet for explicit finite difference. The values inside the bold boxes can be changed and the result plotted in a chart. Figure 7 shows the equivalent spreadsheet with the formulae displayed.

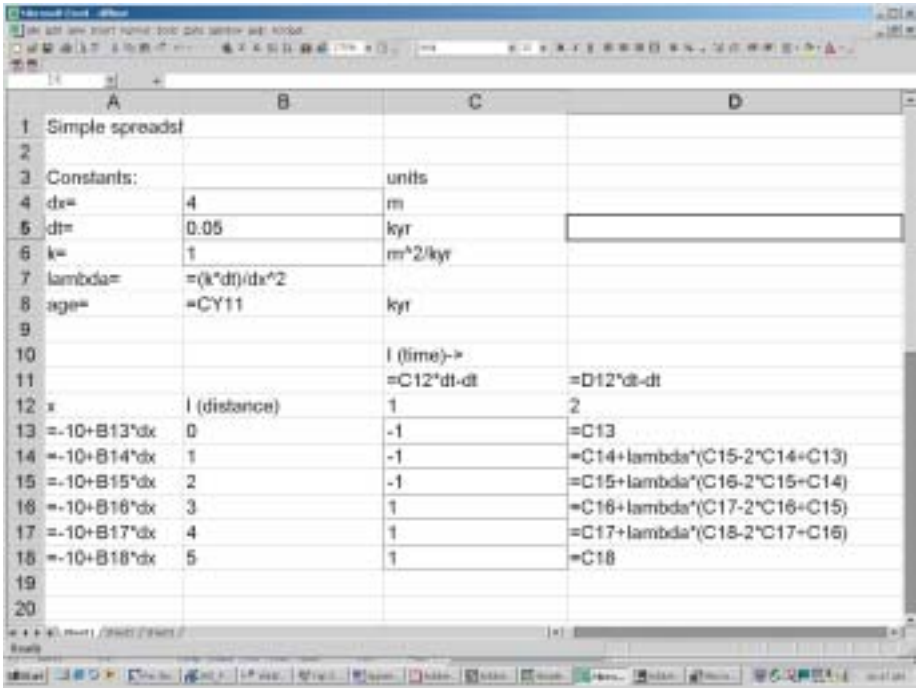

	A	B	C	D
1	Simple spreadsh			
2				
3	Constants:		units	
4	dx=	4	m	
5	dt=	0.05	kyr	
6	k=	1	m^2/kyr	
7	lambda=	=(k*dt)/dx^2		
8	age=	=CY11	kyr	
9				
10			I (time)->	
11			=C12*dt-dt	=D12*dt-dt
12	x	I (distance)	1	2
13	=-10+B13*dx	0	-1	=C13
14	=-10+B14*dx	1	-1	=C14+lambda*(C15-2*C14+C13)
15	=-10+B15*dx	2	-1	=C15+lambda*(C16-2*C15+C14)
16	=-10+B16*dx	3	1	=C16+lambda*(C17-2*C16+C15)
17	=-10+B17*dx	4	1	=C17+lambda*(C18-2*C17+C16)
18	=-10+B18*dx	5	1	=C18
19				
20				

Figure 7: Example Microsoft Excel Spreadsheet for explicit finite difference with formulae shown.

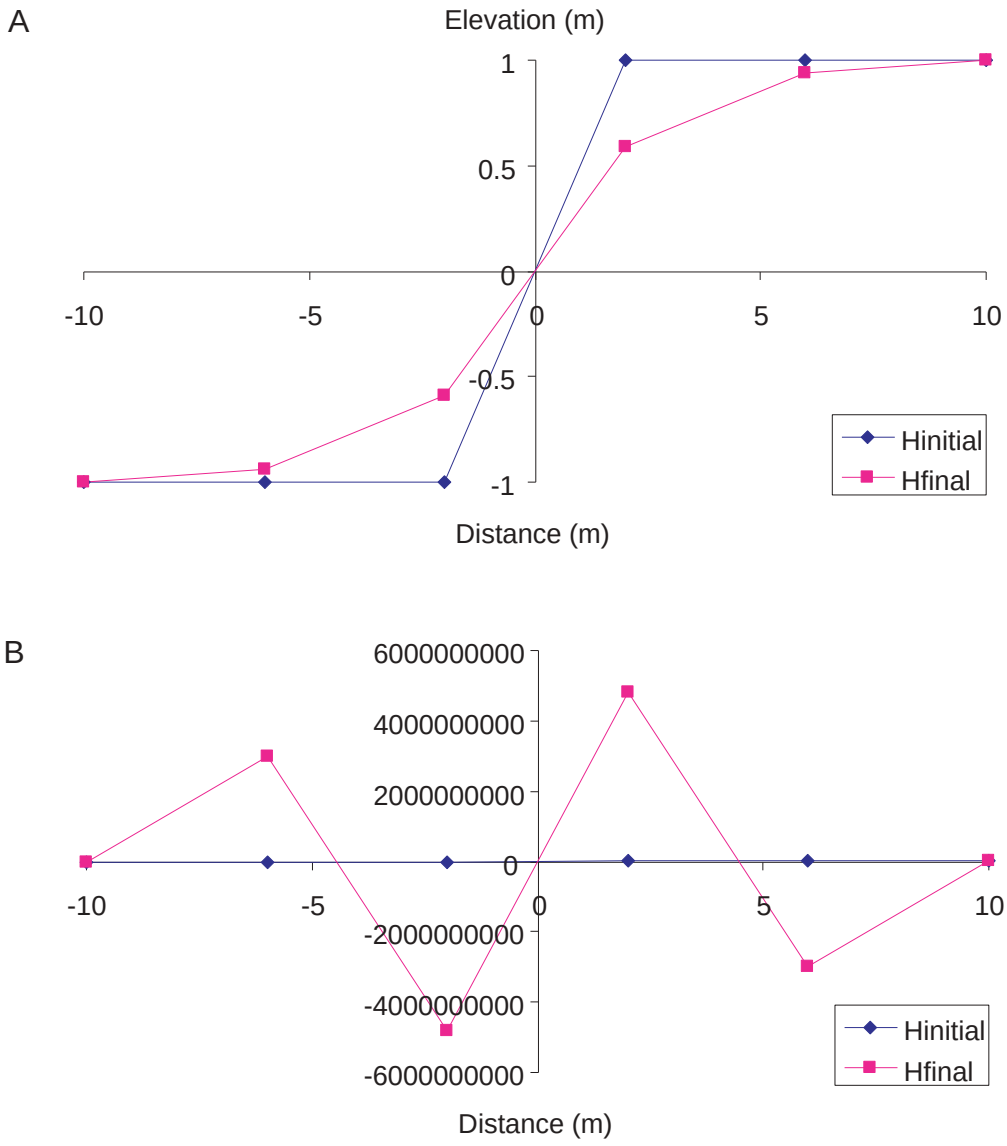

Figure 8: Microsoft Excel plots showing the initial and final profiles determined using the sample spreadsheet (Figures 6 and 7). A) Diffusion erosion solution for degraded step; 1-D explicit finite difference technique, $t = 5$ kyr, $\kappa = 1\text{m}^2/\text{kyr}$. B) Unstable diffusion erosion solution for degraded step; 1-D explicit finite difference technique, $t = 1000$ kyr, $\kappa = 1\text{m}^2/\text{kyr}$ (with a large $\lambda = 0.625$; exceeding the stability criterion).

5 References

Arrowsmith, J R., *Coupled Tectonic Deformation and Geomorphic Degradation along the San Andreas Fault System*, Ph.D. dissertation, 356 pp., Stanford University, June 1995.

Avouac, J. P., Analysis of scarp profiles: evaluation of errors in morphologic dating, *Journal of Geophysical Research*, *98*, 6745-6754, 1993.

Carslaw, H. S., Jaeger, J. C., *Conduction of heat in solids*, 510 p., Oxford, Clarendon Press, 1959.

Chapra, S. C., P. C. Canale, *Numerical Methods for Engineers*, 812 p., McGraw-Hill, San Francisco, 1988.

Ferziger, J. H., *Numerical Methods for Engineering Application*, 270 p., Wiley, New York, 1981.

Hanks, T. C., The age of scarplike landforms from diffusion-equation analysis, in Noller, J. S., Sowers, J. M., and Lettis, W. R., eds., *Quaternary Geochronology*, AGU Reference Shelf, *4*, 313-338, 2000.

Hanks, T. C. and D. J. Andrews, Effect of far-field slope on morphologic dating of scarplike landforms, *Journal of Geophysical Research*, *94*, 565-573, 1989.

Hanks, T. C., R. C. Bucknam, K. R. Lajoie and R. E. Wallace, Modification of wave-cut and fault-controlled landforms, *Journal of Geophysical Research*, *89*, 5771-5790, 1984.